



## Magnetic, spectroscopic and structural properties of a copper cyclic compound

Zhengzhong Lin, Suyan Chen, Zhuzhi Lai, Yingying Wang & Shaoyan Yang

To cite this article: Zhengzhong Lin, Suyan Chen, Zhuzhi Lai, Yingying Wang & Shaoyan Yang (2015) Magnetic, spectroscopic and structural properties of a copper cyclic compound, Journal of Coordination Chemistry, 68:12, 2121-2129, DOI: [10.1080/00958972.2015.1038785](https://doi.org/10.1080/00958972.2015.1038785)

To link to this article: <http://dx.doi.org/10.1080/00958972.2015.1038785>



Accepted author version posted online: 07 Apr 2015.  
Published online: 30 Apr 2015.



Submit your article to this journal [↗](#)



Article views: 50



View related articles [↗](#)



View Crossmark data [↗](#)

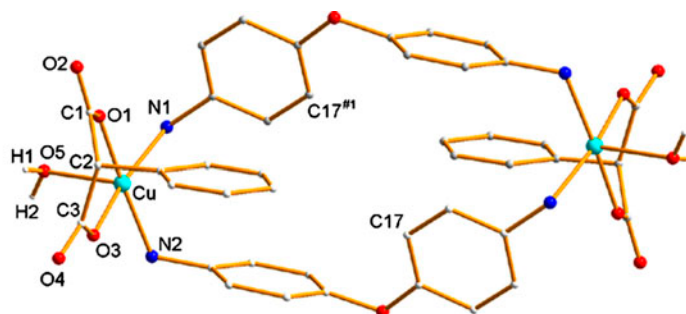
## Magnetic, spectroscopic and structural properties of a copper cyclic compound

ZHENGZHONG LIN\*<sup>†</sup>, SUYAN CHEN<sup>†</sup>, ZHUZHI LAI<sup>‡</sup>, YINGYING WANG<sup>†</sup> and SHAOYAN YANG<sup>†</sup>

<sup>†</sup>College of Food and Biological Engineering, Jimei University, Xiamen, China

<sup>‡</sup>College of Chemistry & Chemical Engineering, Xiamen University, Xiamen, China

(Received 4 January 2015; accepted 18 March 2015)



A new compound  $[\text{Cu}(\text{oda})(\text{pmal})(\text{H}_2\text{O})]_2 \cdot 4\text{H}_2\text{O}$  assembled from phenylmalonic acid ( $\text{H}_2\text{pmal}$ ), 4,4'-diaminodiphenyl ether (oda) and Cu(II) was synthesized under mild conditions in solution. Its structure was determined by X-ray single crystal diffraction. The structure is characteristic of neutral cyclic dimeric molecules which further aggregate through hydrogen bonds and  $\pi$ - $\pi$  interactions to form a 3-D supramolecular network. The compound was also characterized by UV-vis, TG-DSC, XRD, ESR and magnetic susceptibility.

**Keywords:** Copper; Diaminodiphenyl ether; Phenylmalonic acid; Crystal structure; Cycle

### 1. Introduction

Cyclic compounds are important in molecular recognition of electron-rich aromatic guests [1], molecular anion sensing [2] and antimicrobial reagents [3–5]. The choice of organic components is a key issue in the design of species with specific cyclic structure and functional features. The derivatives of oda (4,4'-diaminodiphenyl ether, figure 1), especially Schiff bases, are excellent candidates for the rational design of cyclic compounds. The flexibility of such ligands favors assembly of multi-meric  $[\text{M}_m\text{L}_n]$  cyclic species with versatile

\*Corresponding author. Email: [linzz@jmu.edu.cn](mailto:linzz@jmu.edu.cn)

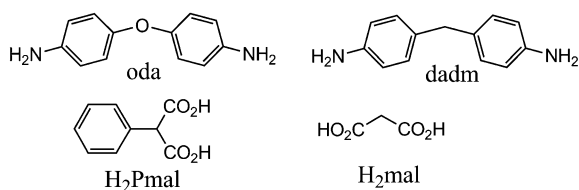


Figure 1. The structures of the ligands.

structures and useful properties. A number of complexes [6–12] based on Schiff bases of oda have been described. However, to the best of our knowledge, examples of cyclic compounds using oda itself are rare [13]. The terminal amino groups in oda facilitate formation of hydrogen bonds which are very important for molecular recognition [14, 15] between receptors and substrates as well as construction [9, 16] of complicated supramolecular arrays. Here we reported a new metallocycle  $[\text{Cu}(\text{oda})(\text{pmal})(\text{H}_2\text{O})]_2 \cdot 4\text{H}_2\text{O}$  (H<sub>2</sub>pmal represents phenylmalonic acid, figure 1) prepared under mild conditions. Prior to this work, the crystal structures of two analogous metallocycles,  $\{[\text{Cu}(\text{dadm})(\text{H}_2\text{mal})(\text{Cl})] \cdot \text{Cl}\}_2$  [17] and  $[\text{Cu}(\text{dadm})(\text{pmal})(\text{H}_2\text{O})]_2 \cdot 4\text{H}_2\text{O}$  [18] (dadm and H<sub>2</sub>mal represent 4,4'-diaminodiphenylmethane and malonic acid, respectively, shown in figure 1) had been described, but the detailed descriptions of spectroscopic and magnetic properties of such metallocycles have not been reported. In this paper we discuss the spectroscopic properties, including ESR, and the magnetic susceptibility as well as the crystal structure.

## 2. Experimental

### 2.1. Reagents and instruments

All reagents were obtained from commercial sources and used without purification. The IR spectrum was recorded on a JASCO FT/IR480PLUS spectrometer as KBr pellets from 4000 to 400  $\text{cm}^{-1}$ . Elemental analysis was carried out on an Elementar Vario EL III microanalyzer. UV–vis spectra were recorded on a Varian CARY50 spectrometer. TG-DSC analysis was performed at a heating rate of 10  $^\circ\text{C min}^{-1}$  using a SDT Q600 simultaneous TG-DSC instrument. X-ray powder diffraction was carried out using a Panalytical X'pert PRO X diffractometer. Variable temperature magnetic susceptibility (2–300 K) of a polycrystalline sample was measured on a SQUID MPMS XL-7 at a field of 5000 Oe. X-band (9.84 GHz) ESR spectra were recorded with a BRUKER EMX-10/12 spectrometer operating at 100 kHz modulation frequency.

### 2.2. Synthesis of $[\text{Cu}(\text{oda})(\text{pmal})(\text{H}_2\text{O})]_2 \cdot 4\text{H}_2\text{O}$

H<sub>2</sub>pmal (108 mg, 0.6 mmol) in 2 mL EtOH, oda (120 mg, 0.6 mmol) in 5 mL DMF and  $\text{CuCl}_2 \cdot 2\text{H}_2\text{O}$  (102 mg, 0.6 mmol) in 10 mL H<sub>2</sub>O were mixed. Aqueous NaOH (0.8 mL, 0.4 mol L<sup>-1</sup>) was added dropwise to the mixture until the pH reached 5.0. A green solution was obtained which was further stirred for 5 min and allowed to stand at room temperature for a week. Block-shaped green crystals of  $[\text{Cu}(\text{oda})(\text{pmal})(\text{H}_2\text{O})]_2 \cdot 4\text{H}_2\text{O}$  were obtained.

Yield: 237 mg (80%). Anal. Calcd (%) for  $C_{42}H_{48}Cu_2N_4O_{16}$  C, 50.86; N 5.65; H, 4.88. Found (%): C 51.08; N 5.71; H 4.67. IR (KBr,  $\nu/cm^{-1}$ ): 3370(m), 3248(m), 3146(s), 1624(vs), 1499(s), 1411(s), 1255(s), 1220(m). Attempts to obtain single crystals of the complexes with various other metal ions using the same method failed.

### 2.3. X-ray crystal structure determination

A single crystal with approximate dimensions (mm) of  $0.11 \times 0.08 \times 0.04$  was placed on the tip of a glass fiber and mounted on a Bruker Smart APEX CCD diffractometer equipped with graphite-monochromated MoK $\alpha$  radiation ( $\lambda = 0.71073 \text{ \AA}$ ) for data collection using an  $\omega$  scan mode at 298 K. Corrections for multi-scan absorption were applied. The structure was solved by direct methods using SHELXS-97 and refined with SHELXL-97 [19]. The non-hydrogen atoms were refined anisotropically. The hydrogens attached to the framework were generated theoretically and refined as riding atoms. The hydrogens on solvent oxygens were located by using the PLATON toolkit [20]. The structure was refined using a full-matrix least-squares refinement on  $F^2$ . Total, independent and observed reflections with  $I > 2\sigma(I)$  were 12,234, 4815 and 4428 respectively with  $R_{int} = 0.0432$ . The final cycle of refinement converged to  $R = 0.0545$  ( $I > 2\sigma(I)$ ),  $wR = 0.1169$  ( $w = 1/[\sigma^2(F_o^2) + (0.03P)^2 + 27P]$ ), where  $P = (F_o^2 + 2F_c^2)/3$ ,  $S = 0.985$ ,  $\mu = 1.109 \text{ mm}^{-1}$ ,  $(\Delta/\sigma)_{max} = 0.000$ ,  $(\Delta\rho)_{max} = 0.839$  and  $(\Delta\rho)_{min} = -0.489 \text{ e/\AA}^3$ .

## 3. Results and discussion

### 3.1. Solubility and conductivity of the compound

The as-prepared compound is stable in air and soluble in DMF, but insoluble in  $H_2O$  or EtOH. The conductivity of the compound and  $CuCl_2 \cdot 2H_2O$  in DMF solution ( $2 \text{ mg mL}^{-1}$ ) is  $5.38$  and  $2420 \text{ }\mu\text{S cm}^{-1}$ , respectively, suggesting that the compound remains intact after dissolution.

### 3.2. Description of the structure

The compound crystallizes in the monoclinic space group  $C2/c$  with crystal parameters of  $a = 13.664(3) \text{ \AA}$ ,  $b = 10.112(3)$ ,  $c = 30.617(8) \text{ \AA}$ ,  $\beta = 101.924(5)^\circ$ ,  $V = 4139(2) \text{ \AA}^3$ ,  $Z = 4$ , formula  $C_{42}H_{48}Cu_2N_4O_{16}$ , formula weight 992 and  $D_c = 1.592 \text{ g}\cdot\text{cm}^{-3}$ . The cell parameters are almost identical to those in Ref. [18], but different from those in ref [17] for related compounds. The asymmetric unit is illustrated in figure 2 and selected bond lengths and angles are listed in table 1. The molecular structure of the compound is characteristic of a discrete neutral metallocycle (figure 3) composed of two Cu(II) ions, two  $\text{pmal}^{2-}$  anions, two oda ligands and two coordinated water molecules. The conformation of the metallocycle is similar to that of the two examples reported in the literature [17, 18]. Each Cu(II) adopts a square pyramidal geometry which is confirmed by the Addison parameter [21] of 0.08. The coordinated water O5 occupies the apex position. The Cu–O5 bond length is longer than that of the other bonds between the Cu(II) ions and the equatorial atoms. Both carboxylates in the  $\text{pmal}^{2-}$  groups are monodentate, however the C1–O1 distance is larger than that of C2–O3. This difference is presumably due to the formation of the hydrogen

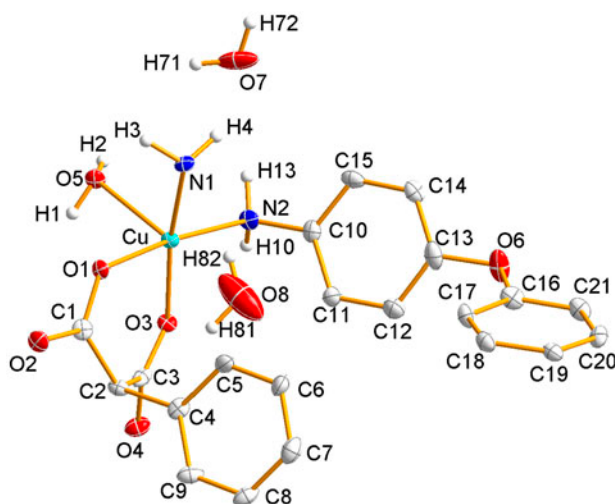


Figure 2. A thermal ellipsoid drawing (30% probability level) of the asymmetric unit of the complex. Only hydrogens on oxygen and nitrogen are shown for clarity.

bond O5–H1 $\cdots$ O1 (table 2) which weakens the C1–O1 bond. The coordination motifs of Cu(II) and carboxylate ions are fundamentally similar to those of the reference compounds [17, 18].

The O6–C16 distance of 1.378(4) Å and the O6–C13 of 1.403(4) Å are both in the typical range of C–O bond lengths (O6 is the atom connecting two phenyl rings in oda). They are both shorter than the corresponding distance of  $\sim$ 1.51 Å in the model compound [18].

The separation between two Cu(II) ions within the macrocyclic complex is 11.173(3) Å. The distance between C17 and C17<sup>#1</sup>, 4.15(1) Å, can be defined as the pore size within the macrocycle. Generally the macrocycle is a bit larger than its analogs [17], as reflected by the shorter Cu $\cdots$ Cu distance (10.83 Å) and pore size (4.09 Å) of the known complexes [17]. In addition, the dihedral angle of 69.8(1) $^\circ$  between the two phenyl rings in one oda is smaller than the corresponding literature value of 88.1 $^\circ$  [17]. The difference in dihedral angle is presumably due to the introduction of the aromatic rings in the pmal<sup>2-</sup> groups. The phenyl rings in one oda are parallel to the corresponding phenyl rings in the other oda

Table 1. Selected bond lengths and angles ( $^\circ$ ) for the compound.

Lengths (Å)		Angles ( $^\circ$ )	
Cu–O1	1.935(2)	O1–Cu–O3	91.67(9)
Cu–O3	1.950(2)	O1–Cu–N2	172.8(1)
Cu–N2	2.030(3)	O3–Cu–N2	84.2(1)
Cu–N1	2.047(3)	O1–Cu–N1	86.5(1)
Cu–O5	2.242(2)	O3–Cu–N1	168.2(1)
O1–C1	1.300(4)	N2–Cu–N1	96.4(1)
O2–C1	1.213(4)	O1–Cu–O5	88.77(9)
O3–C3	1.268(4)	O3–Cu–O5	101.88(9)
O4–C3	1.247(4)	N2–Cu–O5	97.8(1)
O6–C16	1.378(4)	N1–Cu–O5	89.8(1)
O6–C13	1.403(4)		

Note: O1, O2, O3 and O4 belong to two carboxylate groups.

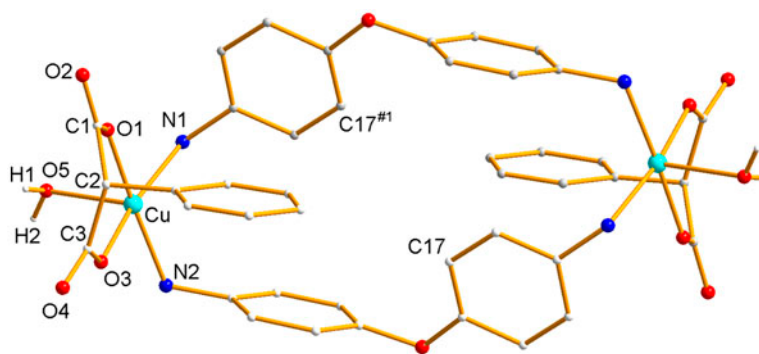


Figure 3. The dimeric macrocyclic structure of the compound. For clarity the hydrogens and lattice water molecules are not shown. Symmetry code: #1  $2-x, 1-y, 2-z$ .

Table 2. Selected hydrogen bonds for the compound.

D-H...A	D-H (Å)	H...A (Å)	D...A (Å)	D-H...A(°)
O5-H1...O1 <sup>#2</sup>	0.84	2.18	2.875(3)	140.8
O5-H2...O4 <sup>#3</sup>	0.84	1.90	2.662(3)	149.8
O7-H72...O4 <sup>#4</sup>	0.86	2.27	2.785(4)	118.6
O8-H81...O5 <sup>#5</sup>	0.85	2.22	3.013(6)	155.9
O8-H82...O4 <sup>#3</sup>	0.85	2.65	3.386(8)	146.6
N1-H4...O7	0.92	2.09	2.903(4)	147.3
N1-H3...O8 <sup>#6</sup>	0.92	2.66	3.538(7)	161.0
N2-H10...O8	0.92	2.14	3.059(6)	175.1
N2-H13...O2 <sup>#7</sup>	0.92	2.15	2.980(4)	149.7

Notes: O7 and O8 are the isolated water oxygen atoms. Symmetry code: #2  $-x, y, -z+3/2$ ; #3  $-x+1/2, y-1/2, -z+3/2$ ; #4  $x, y-1, z$ ; #5  $-x+1/2, y+1/2, -z+3/2$ ; #6  $x-1/2, y-1/2, z$ ; #7  $x+1/2, y-1/2$ .

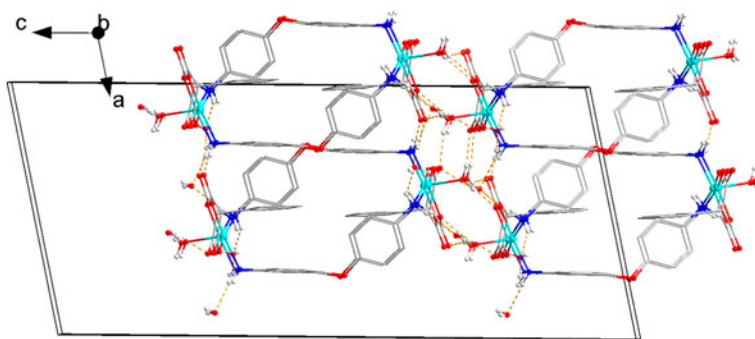


Figure 4. The supramolecular network of the compound showing the hydrogen bonds which are represented by dashed lines.

molecule, and the two phenyl rings of the  $\text{pmal}^{2-}$  groups within one macrocycle are also parallel to each other.

The supramolecular network of the compound is directed by a combination of effects including strong face-to-face  $\pi$ - $\pi$  stacking interactions and hydrogen bonds (figure 4). The

benzene rings from  $\text{pmal}^{2-}$  and oda groups are alternately arranged along the  $(-411)$  direction to form  $\pi$ - $\pi$  stacking interactions (centroid-to-centroid distance is 3.58 Å with the dihedral angle near 5.2°). A similar  $\pi$ - $\pi$  stacking system is also observed in one of the reference compounds [18], but not in the other [17], which indicates that the introduction of  $\text{pmal}^{2-}$  groups has affected the self-assembly behavior between the metallocycles. The oxygens from carboxylate, coordinated water, lattice water and the amino groups are all involved in the formation of hydrogen bonds which are listed in table 2.

The homogeneity of the compound is confirmed by X-ray powder diffraction in which both the angles ( $2\theta$ ) and the strength of the experimental pattern are in agreement with that of the calculated pattern [22].

### 3.3. Absorption spectra

Absorption spectra (figure 5) of the mixtures of  $\text{H}_2\text{pmal}$  and oda with and without Cu(II) ions were scanned under the same conditions as used in the preparation of the complex. The solution without Cu(II) ions shows a  $\pi$ - $\pi^*$  transition at 280 nm ( $\epsilon = 0.95 \times 10^{-4} \text{ L mol}^{-1} \text{ cm}^{-1}$ ). The addition of Cu(II) ions significantly enhances the  $\pi$ - $\pi^*$  transition, which indicates an interaction between Cu(II) ions and the ligand mixtures.

### 3.4. TG-DSC analysis

The results of TG-DSC measurements under normal atmosphere, as shown in figure 6, reveal that the first weight loss of 8.2% from 100 to 140 °C corresponds to loss of two lattice waters per asymmetric unit (calculated: 7.2%) accompanying a weak endothermic peak. The second weight loss from 200 to 400 °C corresponds to loss of coordinated water, oda and  $\text{pmal}^{2-}$  ligands. However, the observed weight loss (31%) is much lower than the expected value (calcd 80% weight loss), which may be due to the retention of solid carbon residue. The subsequent weight loss (40%) from 420 to 550 °C may be attributed to the oxidation of the carbon residue (calcd 49% weight loss) with a strong exothermic peak. The compound finally transforms to CuO with the total weight loss of 85.8% (calculated: 84.0%).

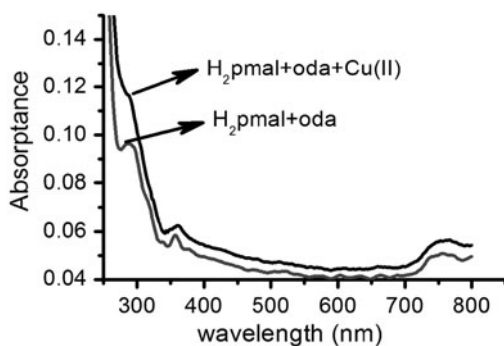


Figure 5. The absorption spectra of the ligand mixture ( $\text{H}_2\text{pmal}$  and oda) with and without the addition of Cu(II) ions at  $1.0 \times 10^{-5} \text{ mol L}^{-1}$ .

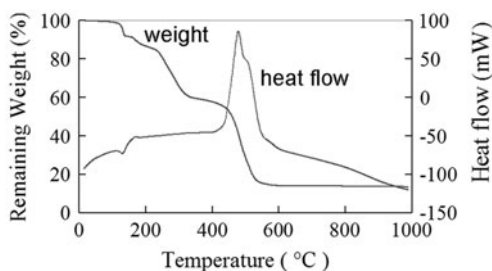


Figure 6. TG-DSC data for the compound.

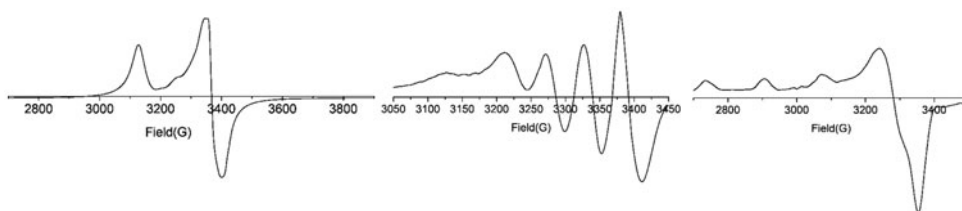


Figure 7. ESR spectra of the compound. Left: polycrystalline at room temperature; middle: in solution at room temperature; right: in frozen solution at 90 K.

### 3.5. ESR spectra

The ESR spectra (figure 7) of the compound were recorded in the polycrystalline state and in DMF solution. The polycrystalline ESR spectrum at 300 K has almost the same signal as at 90 K. Both lack hyperfine structure, giving  $g_{zz} = 2.2493$ ,  $g_{yy} = 2.0889$ ,  $g_{xx} = 2.0448$  and  $g_{ave} = 2.1277$ . The fact that  $g_{zz} > g_{xx} \approx g_{yy}$  confirms a distorted and elongated Cu(II) octahedral or square pyramidal stereochemistry with a  $d(x_2 - y_2)^1$  ground state [23]. The signal at ca. 3350 G suggests the presence of spin-spin interaction ( $\Delta MS = \pm 1$  allowed transitions) [24]. In addition the compound gives a  $G$  value = 3.73 ( $< 4$ ) ( $G = (g_{\parallel} - 2)/(g_{\perp} - 2)$ ), indicating the presence of spin exchange coupling between Cu(II) ions [25]. In DMF solution, an isotropic spectrum at 300 K containing only four copper hyperfine lines is observed with  $g = 2.1233$ ,  $A = 54G$ . The frozen solution spectrum at 90 K shows the typical Cu(II) signals with four hyperfine peaks in the parallel region derived from coupling of the Cu(II) nucleus and the unpaired electrons. The spectral parameters,  $g_{zz} = 2.2538$ ,  $A_{zz} = 170G$ ,  $g_{yy} = 2.0530$ ,  $g_{xx} = 2.0498$ ,  $A_{xx} = A_{yy} = 18G$ , are similar to those reported for copper(II) complexes with a square pyramidal geometry [26].

### 3.6. Magnetic susceptibility

The temperature dependence of  $\chi_m T$  and  $\chi_m^{-1}$  ( $\chi_m$ : molar magnetic susceptibility) of the compound are plotted in figure 8. With decreasing temperature, the  $\chi_m T$  value remains constant down to 100 K where it begins decreasing slowly and then decreases sharply below 20 K to reach  $0.47 \text{ cm}^3 \text{ mol}^{-1} \text{ K}$  at 2 K. Curie-Weiss fitting gives the values of  $C = 0.834(1) \text{ cm}^3 \text{ mol}^{-1} \text{ K}$  and  $\theta = -1.69(6) \text{ K}$  in which  $C$  is the Curie constant



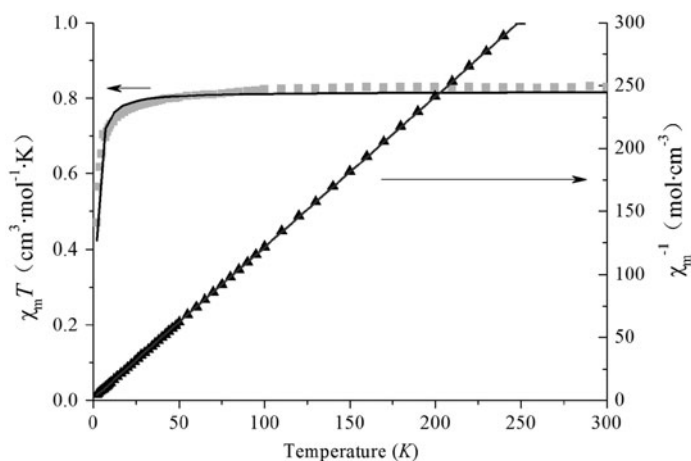


Figure 8. Temperature dependences of  $\chi_M T$  and  $\chi_M^{-1}$  of the compound. Black lines correspond to the best agreement with Bleaney–Bowers equation and Curie–Weiss law (see text) for  $\chi_M T$  and  $\chi_M^{-1}$ , respectively.

( $C = N\beta^2 g^2 S(S+1)/3k$ ) and  $\theta$  is the Weiss temperature. The small negative value of  $\theta$  reveals the occurrence of weak antiferromagnetic interactions between Cu(II) spin units. The magnetic susceptibility data were analyzed by using the Bleaney–Bowers equation on the dinuclear Cu(II) model [27, 28].

$$\chi_M = \frac{2Ng^2\beta^2}{kT} \times \frac{e^{J/kT}}{1 + 3e^{J/kT}}$$

The best agreement is obtained with  $g = 2.112(3)$ ,  $J = -1.08(3) \text{ cm}^{-1}$ , which indicates that the magnetic exchange between the adjacent Cu(II) ions is very weak. This is consistent with the long interatomic Cu··Cu distance.

#### 4. Conclusions

An air stable Cu(II) macrocyclic compound  $[\text{Cu}(\text{oda})(\text{pmal})(\text{H}_2\text{O})_2] \cdot 4\text{H}_2\text{O}$  has been synthesized and characterized. X-ray crystal analysis reveals that the compound has a dinuclear cyclic configuration with an intramolecular Cu··Cu distance of 11.173(3) Å and a pore size of 4.15(1) Å. The 3D supramolecular network is constructed via hydrogen bonds and  $\pi$ – $\pi$  stacking interactions. The compound loses its organic component by stages upon heating as evidenced by TG-DSC analysis. The ESR spectra reveal coordination of Cu(II) ions and the presence of spin exchange coupling between Cu(II) ions. The magnetic susceptibility indicate weak antiferromagnetic interactions between Cu(II) ions.

#### Disclosure statement

No potential conflict of interest was reported by the authors.

## Funding

This work was supported by SRF for ROCS, SEM [grant number 201210100002]; the Foundation for Innovative Research Team of Jimei University, China [grant number 2010A007]; National Undergraduate Training Programs for Innovation and Entrepreneurship [grant number 201410390009]; the Science and Technology Planning Project of Fujian Province, China [grant number 2014Y0045]; and the Educational Commission of Fujian Province [grant number JB111104].

## Supplementary data

CCDC 1,018,504 contains the supplementary crystallographic data of this paper. These data can be obtained free of charge from the Cambridge Crystallographic Data Center via [www.ccdc.cam.ac.uk/data\\_request/cif](http://www.ccdc.cam.ac.uk/data_request/cif).

## References

- [1] J.H. Luo, M.C. Hong, R.H. Wang, R. Cao, Q. Shi, J.B. Weng. *Eur. J. Inorg. Chem.*, **2003**, 1778 (2003).
- [2] R.V. Slone, D.I. Yoon, R.M. Calhoun, J.T. Hupp. *J. Am. Chem. Soc.*, **1**, 1995 (1813).
- [3] J. Choi, J. Kim, K. Kim, S.T. Yang, J.I. Kim, S. Jon. *Chem. Commun.*, 1151 (2007).
- [4] I. Tsyba, B.B. Mui, R. Bau, R. Noguchi, K. Nomiya. *Inorg. Chem.*, **42**, 8028 (2003).
- [5] N. Nishat, D. Rahis Ud, S. Dhyani. *J. Coord. Chem.*, **62**, 996 (2009).
- [6] M. Vazquez, M.R. Bermejo, M. Licchelli, A.M. Gonzalez-Noya, R.M. Pedrido, C. Sangregorio, L. Sorace, A.M. Garcia-Deibe, J. Satunartin. *Eur. J. Inorg. Chem.*, **2005**, 3479 (2005).
- [7] Z.L. Chu, W. Huang. *J. Mol. Struct.*, **837**, 15 (2007).
- [8] C. He, C.Y. Duan, C.J. Fang, Q.J. Meng. *J. Chem. Soc., Dalton Trans.*, 2419 (2000).
- [9] N. Yoshida, H. Oshio, T. Ito. *J. Chem. Soc., Perkin Trans.*, **2**, 975 (1999).
- [10] H.J. Yun, S.H. Lim, S.W. Lee. *Polyhedron*, **28**, 614 (2009).
- [11] D. Guo, K.L. Pang, C.Y. Duan, C. He, Q.J. Meng. *Inorg. Chem.*, **41**, 5978 (2002).
- [12] H.B.T. Jeazet, K. Gloe, T. Doert, O.N. Kataeva, A. Jäeger, G. Geipel, G. Bernhard, B. Büechner, K. Gloe. *Chem. Commun.*, **46**, 2373 (2010).
- [13] R.H. Wang, M.C. Hong, J.H. Luo, R. Cao, J.B. Weng. *Eur. J. Inorg. Chem.*, **2002**, 3097 (2002).
- [14] Y. Zhao, J. Gu, Y.C. Yang, H. Shi, H.Y. Zhu, R. Huang, B. Jing. *Res. Chem. Intermed.*, **35**, 597 (2009).
- [15] K. Uemura, S. Kitagawa, M. Kondo, K. Fukui, R. Kitaura, H.C. Chang, T. Mizutani. *Chem. Eur. J.*, **8**, 3586 (2002).
- [16] N. Yoshida, H. Oshio, T. Ito. *J. Chem. Soc., Perkin Trans.*, **2**, 1674 (2001).
- [17] Y.G. Zhang, M. Nishiura, J.M. Li, D. Wei, T. Imamoto. *Inorg. Chem.*, **38**, 825 (1999).
- [18] Z.Z. Lin, S.Y. Chen, C.Y. Zhou, Y.P. Zhang, Z.Z. Lai. *J. Chem. Chin. J. Struct. Chem.*, **32**, 381 (2013).
- [19] G.M. Sheldrick *Acta Cryst.*, **A64**, 112 (2008).
- [20] L.A. Spek. *Multipurpose Crystallographic Tool*, Utrecht University, The Netherlands (1999).
- [21] A.W. Addison, T.N. Rao, J. Reedijk, J. van Rijn, G.C. Verschoor. *J. Chem. Soc., Dalton Trans.*, 1349 (1984).
- [22] Mercury for windows (version 3.5.1), CCDC, University of Cambridge, Cambridge (2015).
- [23] M. Murali, M. Palaniandavar, T. Pandiyan. *Inorg. Chim. Acta*, **224**, 19 (1994).
- [24] M. Julve, M. Verdager, M.F. Charlot, O. Kahn, R. Claude. *Inorg. Chim. Acta-Art. Lett.*, **82**, 5 (1984).
- [25] I.M. Procter, B.J. Hathaway, P. Nicholls. *J. Chem. Soc. A*, 1678 (1968).
- [26] R.N. Patel, N. Singh, K.K. Shukla, U.K. Chauhan, J. Niclos-Gutierrez, A. Castineiras. *Inorg. Chim. Acta*, **357**, 2469 (2004).
- [27] O. Kahn. *Molecular Magnetism*, p. 380, VCH, New York (1993).
- [28] B. Bleaney, K.D. Bowers. *Proc. R. Soc. London, Ser. A*, **214**, 451 (1952).